Lab on a Chip

Multi-Cellular 3D Human Primary Liver Cell Culture Elevates Metabolic Activity Under Fluidic Flow

Journal:	*Lab on a Chip*
Manuscript ID:	LC-ART-02-2015-000237
Article Type:	Paper
Date Submitted by the Author:	27-Feb-2015
Complete List of Authors:	Esch, Mandy; Cornell Nanofabrication Facility, Prot, Jean-Matthieu; Cornell University, BME Wang, Ying; Cornell University, BME Miller, Paula; Cornell University, BME Llamas-Vidales, Jose; RegeneMed Inc., Naughton, Brian; RegeneMed Inc., Applegate, Dawn; RegeneMed Inc., Shuler, Michael; Cornell University, Department of Chemical and Biomolecular Engineering

Multi-Cellular 3D Human Primary Liver Cell Cultures Elevate Metabolic Activity Under Fluidic Flow

Mandy B. Esch,[1] Jean-Matthieu Prot,[1] Ying I. Wang,[1] Paula Miller,[1] Jose Ricardo Llamas-Vidales,[2] Brian A. Naughton,[2] Dawn R. Applegate,[2] Michael L. Shuler[1,*]

1) Department of Biomedical Engineering, 305 Weill Hall, Cornell University, Ithaca, NY, 853, United States

2) RegeneMed Inc., 9855 Towne Centre Drive Suite 200, San Diego, CA 9, USA

**) Corresponding author*

Keywords: Bioreactor, gravity driven flow, microfluidic cell culture, hepatocyte function, 3D environment

Abstract :

Predicting drug-induced liver injury with in vitro cell culture models more accurately would be of significant value to the pharmaceutical industry. To this end we have developed a low-cost liver cell culture device that creates fluidic flow over a 3D primary liver cell culture that consists of multiple liver cell types, including hepatocytes and non-parenchymal cells (fibroblasts, stellate cells, and Kupffer cells). We tested the performance of the cell culture under fluidic flow for 14 days, finding that hepatocytes produced albumin and urea at elevated levels compared to static cultures. Hepatocytes also responded with induction of P450 (CYP1A1 and CYP3A4) enzyme activity when challenged with P450 inducers, although we did not find significant differences between static and fluidic cultures. Non-parenchymal cells were similarly responsive, producing interleukin 8 (IL-8) when challenged with 10 μM bacterial lipoprotein (LPS). To create the fluidic flow in an inexpensive manner, we used a rocking platform that tilts the cell culture devices at angles between ±12°, resulting in a periodically changing hydrostatic pressure drop and bidirectional fluid flow (average flow rate of 650 μL/min, and a maximum shear stress of 0.64 dyne/cm^2). The increase in metabolic activity is consistent with the hypothesis that, similar to unidirectional fluidic flow, primary liver cell cultures derived from human tissues increase their metabolic activity in response to bidirectional fluidic flow. Since bidirectional flow drastically changes the behavior of other cells types that are shear sensitive, the finding that bidirectional flow increases the metabolic activity of primary liver cells also supports the

theory that this increase in metabolic activity is likely caused by increased levels of gas and metabolite exchange or by the accumulation of soluble growth factors rather than by shear sensing. Our results indicate that device operation with bi-directional gravity-driven medium flow supports the 14-day culture of a mix of primary human liver cells with the benefits of enhanced metabolic activity. Our mode of device operation allows us to evaluate drugs under fluidic cell culture conditions and at low device manufacturing and operation costs.

Introduction:

Drug hepatotoxicity is one of the most common reasons for drug attrition during clinical trials.[1] One of the reasons for the failure to predict drug toxicity accurately despite extensive testing is that animals and in vitro tissues do not recapitulate human tissues, metabolism and relevant inter-organ interactions as accurately as needed. In vitro cell culture conditions that increase the sensitivity of liver cells to adverse drug actions could help in identifying drugs that will be successful in later clinical trials more easily.

Recreating the full complexity of liver tissue in vitro is important for drug screening because depending on the nature of the drug challenge, liver injury is the result of complex tissue responses that involves multiple liver cell types [2] and sometimes even multiple organs.[3] In an effort to detect idiosyncratic hepatotoxicity in vitro, Kostadinova et al. have developed a technique that allowed the culture of multiple primary liver cell types such as hepatocytes and non-parenchymal liver cells (a mixture of fibroblasts, stellate cells and Kupffer cells) within a 3D scaffold. This complex 3D multi-cell type culture has been tested extensively under static conditions in 2010,[2] showing that the culture achieves the detection of idiosyncratically toxic drugs. Here we subject, for the first time, multi-cellular 3D liver cell cultures consisting of primary hepatocytes and non-parenchymal cells (fibroblasts, stellate cells, and Kupffer cells) to recirculating fluidic flow that provides moderate levels of shear.

It has previously been found that culturing primary hepatocytes under fluidic flow that does not create shear exceeding harmful threshold values could be of advantage in the drug testing process.[4-7] When primary hepatocytes grow in 2D or 3D cultures that are perfused, they increase their urea production beyond the relatively low levels seen in static culture.[4,6,7] This observation is true regardless of the hepatocyte source - animal or human.[8-11] In addition, some authors have shown that when cultures of primary heptocytes of rat and human origin were perfused with medium, the cells also responded to fluidic flow by activating P450 enzymes at a measurably higher level than did comparable static cultures.[11,12] This result could indicate a lower activation threshold, resulting in

potentially improved predictions of drug-induced liver injury if fluidic cultures were used routinely for drug screening.

Here we place, for the first time, 3D primary liver cell cultures consisting of hepatocytes and non-parenchymal cells (fibroblasts, stellate cells, and Kupffer cells) under recirculating fluidic flow. In the device we create fluidic flow by placing it on a rocking platform that tilts back and forth as previously suggested by Sung et al.[13] The height difference between liquid levels in inlet and outlet causes gravity-driven, periodically changing bidirectional fluid flow. Together the dimensions of the fluidic channel and the amount of tilt of the rocking platform determine the flow rate in the system in a predictable manner.[13] We hypothesized that bidirectional fluidic flow that recirculates the cell culture medium is not detrimental to primary liver cell cultures.

Besides providing a way to test for drug action under fluidic conditions, the device presented here also has practical advantages over other fluidics-based cell culture devices. Since gravity creates the fluid flow, no pumps and tubing are needed to operate the device, allowing us to operate many devices in parallel using a single rocker platform. The experimental setup of the devices is simple, and large-scale screening for drug-induced liver injury under fluidic conditions becomes possible and more cost-effective.

Further, idiosyncratic drug toxicity has also been shown to occur when other organs of the human body such as the GI tract are compromised.[3] For this reason, adding biological complexity to the cell culture environment has the potential to increase the physiologic relevance of hepatocyte responses in vitro. Additional cell types of other organs can be co-cultured in discrete chambers within the cell culture system and allow drugs and metabolites from the liver to interact with them via fluidic streams that recirculate between the cultures. Such co-culture devices replicate some of the complex inter-organ interactions that occur in the human body.[14-26] To realize the potential these multi-organ devices bear, it is important to develop and characterize fluidic cell culture devices that recirculate the medium instead of disposing it after flowing over the cell culture.

Materials and Methods:

1) Device construction

The liver tissue construct was prepared using a 0.42 mm thick, macroporous polymer scaffold that was 6.0 mm in diameter. This scaffold was previously used in static cell cultures by Kostadinova et al..[2] The cell culture

chamber into which we placed this scaffold was constructed from two silicone sheets (each 1 mm thick). We sandwiched a porous polycarbonate membrane between the two sheets and placed the liver tissue scaffold on top of the membrane, so that the 1 mm high chamber walls extended over the scaffold by 0.5 mm (Fig. 1), and a bottom chamber of 1 mm height was created below the cell culture. Fluidic access to both top and bottom chambers was created via fluidic channels.

The silicon gasket that formed the cell culture chamber was sandwiched between two pieces of Veroclear polymer (from Stratasys Ltd., Rhovot, Israel) that were both 3D printed (ObJet, 3D printer, Stratasys Ltd., Rhovot, Israel) with 1 x 1 mm groves that functioned as fluidic channels. Both 3D printed polymer pieces were coated with parylene C, a process that renders their surfaces biocompatible with liver cell culture. The devices were assembled as shown in figure 1 so that the fluidic channels of the top and bottom polymer pieces pass above and below the cell culture chamber. Each channel was connected to it's own set of inlet and outlet chambers (see figure 1).

The cell culture device was constructed from two silicone gaskets with 6 mm punched out holes (Electron Microscopy Sciences, Hatfield, PA, USA), a porous polycarbonate membrane (Sterlitech Corp., catalog # P/N PCT12025100) was sandwiched between the two gaskets, a cell culture scaffold obtained from RegeneMed Inc. (San Diego, CA), and two 3D printed pieces of polymer. The polymer pieces were both designed with Solidworks (SolidWorks Corp., Waltham, MA, USA) and printed with a 3D object printer (ObJet 30Pro, Stratasys Ltd., Rehovot, Israel) using the provided Veroclear polymer. The Veroclear pieces were cured for 48 hours at 40 degree C under vacuum and then coated with 5 g of parylene C using a coater from SCS Equipment (Dallas, TX, USA, Model PDS 2010 Labcoater). The pieces were sterilized in 70% ethanol for 1 hour before and washed with sterile PBS before use with cell cultures.

2) Liver cell culture

Primary human hepatocytes and non-parenchymal cells (a mixture of primary human fibroblasts, stellate cells and Kupffer cells) were obtained from Regenemed Inc. (San Diego, CA). The composition of this mixture of cells was determined by Kostadinova et al.[2] For fluidic cell cultures, non-parenchymal cells (NPC) were seeded onto the 6 mm, round scaffold that was placed into the silicone assembly at a concentration of 150,000 cells per scaffold. The silicon assembly with NPC cell cultures was placed for 7 days in a petri dish in a humidified CO_2 incubator at 37°C and the culture was sustained with medium (# L3SNB-500, RegenMed, San Diego, CA). On day 7,

cryopreserved primary human hepatocytes were thawed and seeded onto the scaffold at a concentration of 500,000 cells per scaffold. After 48 h of cell culture in a petri dish, the silicone assembly was aseptically transferred into the cavity of the bottom polymer piece. The device was closed without encapsulating air bubbles using the top piece. 1 mL of medium was equally distributed between the four reservoirs and renewed at 50% every day for 14 days of cell culture. In parallel to fluidic cell cultures, non-parenchymal cells and hepatocytes were also seeded into transwells containing the same 6.0 mm scaffold. Similar to the method described above, non-parenchymal cells were seeded 7 days prior to hepatocytes. This method was developed earlier and is described in detail by Kostadinova et al.[2]

3) Device operation

The assembled devices with liver cell cultures were transferred into 60 mm sterile petri dishes. The dish was placed onto a rocking platform, which facilitated perfusion by creating a height difference in liquid levels in the two reservoirs connected to each of the two fluidic channels. The rocking platform tilted between angles of ±12° at a rate of 3 cycles per minute (each cycle being 20 seconds), resulting in periodic, bi-directional, gravity-induced medium flow.

4) Determining AST and LDH concentrations

To determine the viability of cells we measured the amounts of cytosolic enzymes [aspartate aminotransferase, (AST) and lactate dehydrogenase (LDH)] in the medium taken from the cell cultures. Testing was performed at the clinical pathology laboratory in the Animal Health Diagnostic Center at Cornell University, using an automated chemistry analyzer (Hitachi Modular P, Roche Diagnostics) with manufacturer's reagents. Both AST and LDH levels allow us to quantify the amount of cell death that occurred over the period between measurements and express albumin and urea production per number of live cells.[26]

5) Determining rates of urea and albumin synthesis

250 μL of cell culture medium were collected from the cell cultures on day 3, 7, and 14 of the cell culture with day 1 corresponding to the first day of cell culture in the device (i.e. under fluidic flow conditions). Urea concentrations in the medium were measured using a DIUR assay kit, which we used as suggested by the manufacturer (BioAssay Systems, Hayward, CA, USA, QuantiChrom catalog #DIUR-500). In short, we transferred

50 μL of medium into the wells of a 96 well plate, added chromogenic reagent that forms a stable colored complex specifically with urea, and measured the optical density of the solution within 5 minutes of adding the chromogenic reagent at 520 nm using a spectrophotometer. The results were compared to a standard curve and are expressed as μg/day/million cells.

Albumin synthesis was evaluated by Enzyme-Linked Immunosorbent Assay (ELISA), using a kit and following the manufacturer's directions (Bethyl Laboratories, Inc., Montgomery, TX, USA, catalog # E80-129). In short, we coated the wells of a 96-well plate with goat anti-human albumin antibody and washed the wells with buffer. We then transferred 100 μL medium taken from the cell culture devices into the wells. After incubation, we added HRP-conjugated goat anti-human antibody to the wells and incubated for 1 hour. Following a washing step with buffer, we added 100 μL of enzyme substrate (tetramethylbenzidine) and incubated for 15 min. After adding stopping solution, we measured the absorbance of the solution using a plate reader at 450 nm.

6) Determining P450 enzyme activity

CYP450 enzyme activity was monitored using Promega Glo assays (Promega Corp., Madison, WI, USA, catalog #V9002 for CYP3A4 and catalog #V8752 for CYP1A1). Briefly the induction reagent (10 μM of rifampicin for CYP3A4 and 1 μM of 3-methyl-cholanthrene for CYP1A1 induction) was diluted in medium and added to the four reservoirs of the devices for 72 hours. We then washed the reservoirs with buffer three times for 5 minutes and subsequently replaced the buffer with IPA-luciferin. We used separate devices for measuring the induction of each enzyme. At the end of the incubation period, medium was collected and transferred into the wells of a 96 well-plate. Detection reagent was added and luminescence was read with a veritas luminometer using the settings provided by the manufacturer. Results were expressed as multiples of the level of induction observed in controls that were not treated with induction reagents. For each induction experiment, one separate device was used for control experiments using vehicle controls, and two devices were induced in parallel for each enzyme, producing two technical replicates per enzyme. In total we conducted three separate experiments with two technical replicates per experiment.

7) Measurement of IL-8 Concentrations

The cell cultures were challenged with 10 μM LPS and IL-8 production was measured using ELISA kits

obtained from Invitrogen Inc. (Camarillo, CA, USA, catalog # KHC0081 and # LHC0061). In summary, 50 µL of medium were transferred to the IL-8 specific antibody-coated wells of a 96 well plate. We then added 50 µL biotinylated anti-IL-8 antibody solution and incubated for 90 min at RT. After washing with buffer and aspirating the solution, we added 100 µL of streptavidin-HRP and incubated for 30 min. After washing and aspirating, we added 100 µL of HRP substrate (tetramethylbenzidine) for 30 min and then 100 µL of stop solution. We read the optical density of the solution at 450 nm using a plate reader.

8) Immunostaining

At the end of the 14 day cell culture period, the devices were disassembled and the cells were fixed for 30 min in 4% paraformaldehyde at room temperature. Following a 3x wash with PBS, we permeabilized the cells by applying 0.5% Triton X100 in PBS for 20 min at room temperature. We then washed the cells with PBS containing 1% of bovine serum albumin (BSA) for 60 minutes at room temperature, and then with PBS without BSA 3 times for 5 minutes each. We used the following antibodies: sheep anti human albumin (Abcam, Cambridge, UK, catalog # ab8940) at a dilution of 1:100, mouse anti human CD68 (Abcam, catalog # ab108403) at a dilution of 1:100, and rabbit anti human CD38 (Abcam, catalog # ab108403) at a dilution of 1:100. After 1 h of incubation, we washed with PBS 3 times for 5 minutes and applied secondary antibodies with fluorescent tags (donkey anti-sheep DyLight 650, Abcam, catalog # ab96942, donkey anti-mouse Alexa 488, Abcam, catalog # ab150105, and donkey anti-rabbit Alexa 555, Abcam, catalog # ab150074) at a dilution of 1:50. Nuclei were stained with DAPI.

9) Computational simulation of flow dynamics

The fluidic flow over the cell culture chamber was simulated in 3D with COMSOL Multiphysics 4.3 using the Laminar Flow interface in the Fluid Flow module coupled with the Moving Mesh interface in the Mathematics module. Gravity volume force components parallel to the central channel over the cell culture chamber and perpendicular to the rocker plate, respectively, were applied as functions of the time-dependent tilting angle to model the effects of the back and forth motion of the rocker platform. The fluid levels in reservoirs fluctuate over time. To follow the fluid motion with the moving mesh, the mesh velocity of the free surfaces (the fluid/air interface in the reservoirs) were coupled to the fluid motion normal to the surfaces. A time-dependent study was performed with automatic remeshing. The flow rate and the shear stress were analyzed based on the fluid velocity field from

the solution.

10) Statistical Analysis

The data presented in graphs are means of three separate experiments ± standard deviation. Multiple means were compared with a one-way ANOVA, followed by a Bonferroni adjustment for the number of pair-wise comparisons (JMP software). Comparison of two values with each other was performed using Student's t-tests. A p value of < 0.05 was considered significant.

Results:

1) Fluid Flow and Shear Stress

We designed the dimensions of the fluidic channels and the tilting angle of the device so that the provided fluidic flow that was fast enough to allow for sufficient oxygen supply, and that produces shear conditions that have been associated with beneficial effects for hepatocyte cultures. We simulated the fluidic flow in our devices and calculated the average fluid flow rate and maximum shear stress. Since the device continuously rocks back and forth between maximum platform angles of +12° and -12°, the fluid flow rate through the device does not reach a steady state. The periodically changing fluidic flow is shown in figure 2. The average flow rate was determined to be 650 μL/min. The maximum flow rate is reached at the maximum tilting angle because the resulting flow elevates the fluid level in the lower reservoir significantly, resulting in a significant change of the driving pressure drop.

Mathematical simulations of fluid flow in the devices was also conducted to determine the range of shear stress levels the cells undergo when using gravity-induced bidirectional flow. Figure 2 shows that the highest level of shear occurs when the rocking angle is at its maximum, and zero shear occurs at the moment when the rocking angle and fluid levels in the reservoirs cause the fluid flow to change direction. The range of fluid shear is between -0.638 dyne/cm^2 to + 0.638 dyne/cm^2 with '+' and '-' denoting the two different direction. The maximum shear stress occurs in middle of the cell culture chamber (figure 2 (C)). Fluidic flow through the bottom chamber does not create significant amounts of shear stress that acts on the liver cells since the cells are protected from fluidic flow via the porous membrane.

2) Immunostaining of liver cell types and viability

To characterize the 3D liver cell culture after 14 days of culture in the fluidic device, we opened the devices and immunostained the cells with markers that identified hepatocytes, stellate cells, fibroblasts, and Kupffer cells. We found that even though the cell culture was exposed to the described bidirectional flow, the cells still adhere to the 3D scaffold, appearing tissue-like (figure 3 a and b.) and that all cell types that were initially seeded (hepatocytes, stellate cells, Kupffer cells, and fibroblasts) were still present in the culture (figure 3 c and d). We immunostained hepatocytes using anti-albumin antibodies, stellate cells with anti CD68 antibodies, and Kupffer cells with anti CD38 antibodies. Light microscopy images also reveal that fibroblasts had deposited extracellular matrix onto the scaffold, making it possible for hepatocytes and non-parenchymal cells to adhere (images not shown).

To assess the cell's viability throughout the 14-day cell culture under bidirectional fluidic flow, we collected a fraction of the medium every day and measured concentrations of aspartate transaminase (AST) and lactate dehydrogenase (LDH). The cells of both static and dynamic cultures released LDH in low amounts (7-11 ± 5 U/L per device with 650,000 cells), with a slight increase in LDH release to 25 ± 3 U/L per device loaded with 650,000 cells measured on day 14. The cells released slightly more AST than LDH (22-36 ± 9 U/L device loaded with 650,000 cells). According to previous characterization,[26] the overall low concentrations of LDH and AST (both under 30 U/L device loaded with 650,000 cells, indicating a cell death at a rate of less than 10,000 per week) indicate that the cell cultures are viable under bidirectional flow for 14 days and that device operation for at least 14 days is possible.

3) Metabolism

We measured albumin and urea synthesis throughout the 14-day exposure of the liver cell cultures to bidirectional fluidic flow, finding that hepatocytes increase their albumin and urea production significantly when compared to static cultures. Average values of albumin production ranged from 3 to 7 μg per million cells per day with maximum values reaching a 4.5-fold elevation compared to static cell cultures (figure 4 (A)). Albumin production decreased to its lowest level (3 μg per million cells per day) on day 14, but still maintaining increased levels compared to static cultures. Static cultures maintained a much lower level of albumin with values ranging from 1 to 2 μg per million cells per day. The produced albumin was also visible in microscopy images when stained with anti-albumin antibodies (figure 4 (A) and (B)).

Hepatocytes also elevated their synthesis of urea when cultured under bidirectional fluidic flow. Static cultures performed best on day 3 of the culture period with hepatocytes continuously decreasing urea production after day one. In contrast hepatocytes under fluidic conditions the average urea synthesis activity ranged from 200 to 325 μg per million cells per day under fluidic culture (figure 4). Both albumin and urea synthesis took place until the last day of the fluidic cell culture, and preliminary results with culture times that go beyond 14 days suggest that cultures of up to 28 days are possible.

4) Responses to Challenges

To evaluate whether liver cell cultures that are perfused via gravity-driven bidirectional medium flow are suitable for drug testing, we monitored the hepatocytes's capacity to activate CYP1A1 and CYP3A4 enzymes throughout the 14 days of cell culture. Figure 5 shows that both enzymes respond to inducers with a minimum fold change of 140% and a maximum fold change of 440% compared to un-induced controls (figure 5 a and b). The smallest induction occurred for CYP3A4 on day 3 of device operation. However, in contrast to albumin and urea synthesis, the cells did not perform significantly different when compared with static cultures, with the exception of day 3, where the static culture performed slightly better when induced for CYP 1A1.

To assess the ability of the cell culture to respond to bacterial challenges, we measured the concentration of cytokines in the cell culture medium 24 hours after we challenged the cultures with 10 μM LPS. The cells produced the cytokine IL-8 in response to bacterial lipopolysaccharide (LPS) (figure 6). The response was strongest after one week of cell culture and then decreased towards the end of the culture period.

Discussion:

The results obtained in this study suggest that gravity-driven recirculating fluidic flow can be used to sustain 3D primary liver cultures consisting of primary hepatocytes and non-parenchymal cells (fibroblasts, stellate cells and Kupffer cells) for 14 days of cell culture with the benefit of elevated metabolism. The cells released low levels of cytosolic enzymes (AST and LDH), confirming that they retained high levels of viability throughout the operation of the cell culture device. Low levels of cytosolic enzyme in the cell culture medium have previously been correlated with low amounts of hepatocyte death.[26]

The pumpless cell culture device used here has several practical advantages that distinguish it from other typical fluidic devices. The recirculation of medium within the device does not require tubing or any other equipment that drives or regulates fluidic flow. Uncontrolled drug adsorption to the tubing is a source of error in many devices and the presence of tubing can alter experimental results. Because our device does not require the use of tubing such errors can be avoided. In addition, the devices are easy to set up and one can manage many devices at the same time.

The inserts we used to construct the cell culture chamber can easily be modified to create different chamber volumes, providing an inexpensive and simple way to accommodate other tissues or to test hypotheses in which the relative size of tissue is altered. Similarly, modifications of channel widths and heights are possible so that fluid flow rates can reach values needed for other tissues. Channels self-align to chambers since they are printed as continuous channels in hard plastic, and they also provide a bubble trap on the top of the cell culture chamber. We believe that our device is a low-cost alternative that could be used for routine drug screening under fluidic conditions.

In contrast to others who have shown that fluidic flow elevates the metabolism of primary liver cell cultures,[4-12] our devices created recirculating bidirectional fluidic flow instead of non-recirculating unidirectional fluidic flow. Under bidirectional flow as we have used here, primary hepatocytes produced albumin and urea at elevated levels compared to static control tissues. The static control cultures produced albumin levels that were slightly lower, but comparable to those previously measured by Kostadinova et al.[2] The static cultures' urea production, however, was less than half of the levels measured by previously. This difference in metabolism could be the result of donor-to-donor variation. CYP activity induction reached similar levels, whether fluid flow was present or not. After seeding the cells into the fluidic devices, CYP activity induction was initially even lower than that in static cultures. We speculate that this difference occurs because the transfer of the cell culture into the device produces some amount of stress that affects CYP enzymes, perhaps because hepatocytes become temporarily detached from the scaffold.

Our results support the hypothesis that a fluid-driven increase in metabolic activity is likely the result of increased opportunities for gas and metabolite exchange. One of the most plausible explanations is that the rate of metabolism of the naturally highly metabolically active liver cells is limited in static cultures because gas, nutrient and waste product exchange can be mass-transport limited when the cells are cultured in narrow wells. Here we

utilized a flow rate that is high enough to support an increased gas and nutrient exchange.

Shear stress could also play a role in increasing liver cell metabolism, but data that link shear stress and liver cell metabolism have been inconsistent with some studies even showing decreased rates of metabolism when the shear is raised to moderate levels (5-21 dyne/cm^2).[27] In our culture we prevented negative effects that occurs as a result of high shear stress by designing the cell culture chamber and fluidic circuitry so that the cells experienced low levels of shear throughout the culture. Further, since most pores of the macroporous scaffold are populated by cells, fluidic flow through the tissue scaffold is greatly reduced, further decreasing the level of shear that cells farther down in the scaffold experience. The levels we achieved are comparable to those several others have determined to be beneficial to primary liver cells (~0.3 - 5 dyne/cm^2).[28,27,6,7] Even though we used bidirectional fluidic flow to sustain the cell culture, we did not observe significantly different results compared to those reported for unidirectional fluidic flow. This indicates that liver cells do not respond to a periodic change in shear direction in a way that is detrimental to the culture and to toxicity testing.

A third factor that could influence hepatocytes is the presence of biochemical cues that could accumulate at low flow rates if the cells are cultured in recessed wells. A static study by Williams et al. has shown the positive effects of such cues. [29] Biochemical factors released from fibroblasts, such as components of extracellular matrix, contribute to the hepatocyte's attachment to cell culture scaffolds, and it has also been suggested that soluble factors accumulate at the bottom of the cell culture chamber support hepatocyte function in fluidic systems.[8] Here we use a system that provides fluid streams on top of the culture and also at the bottom. In such a system soluble factors would diffuse into the medium stream over time, limiting the effects accumulation of soluble factors in close proximity to the cell culture. However, our cell culture device recirculates 1 mL of cell culture medium constantly, allowing us to keep the liquid-to-cell ratio lower than has been achieved in microfluidic devices that constantly perfuse the culture with fresh medium. This low liquid-to-cell ratio could result in the accumulation of soluble growth factors and their constant recirculation to the cell culture.

One of our goals in conducting this study was to determine whether this mode of fluidic cell culture would be suitable for further development of a more complex body-on-a-chip system that combines GI tract tissue and liver tissue. Combining liver tissue with GI tract tissue has been shown to alter the response of liver tissue to a drug because the GI tract epithelium can contribute additional biochemical cues that occur when the tissue is exposed to drugs.[3] Here, the organ chamber was a scaled down version of the human liver (by a factor of 110,000). However,

even though the tissue was fairly dense we found that the cells did not populate the scaffold in its entirety. The lower cell density will have to be taken into account when incorporating the culture into a body-on-a-chip device that is meant to recreate the in vivo situation in a scaled down format.

Since immunostaining confirmed the presence of all initially seeded cell types, we suggest that they may be suitable to test for hepatotoxicity that occurs idiosyncratically. Idiosyncratic drug toxicity takes place when complex response mechanisms from several cell types synergize and culminate in an adverse reaction of the tissue to a drug. Since this type of toxicity involves multiple cell types and mechanisms that are not easily predicted, it is important to include all major liver cell types within any in vitro cell culture that will be used for drug testing. The cell composition we have used here was used earlier by Kostadinova et al. under static cell culture conditions, and because of its ability to respond in a complex manner, the culture identified several hepatotoxins that have been regarded as indiosyncratic toxins.[2]

Conclusions:

Our fluidic cell culture system supports the 14-day culture of human primary liver tissue that has been shown to identify known idiosyncratic hepatotoxins in an earlier study. The tissue consists of multiple cells types, among them hepatocytes and non-parenchymal cells (fibroblasts, stellate cells and Kupffer cells). Our device is easy to operate since it relies on gravity to create oscillatory bidirectional fluidic flow that enhances the metabolic activity of the tissue. The results discussed here show that bidirectional fluidic flow confers similar benefits to the cell culture as unidirectional flow in terms of ureagenesis and albumin production.

The developed tissue culture can be integrated into more complex body-on-a-chip devices that contain additional tissues representing other organs to simulate organ-organ interactions that are be relevant in causing idiosyncratic hepatotoxicity. However, tissue density and activity are not exactly the same as in vivo and adjustments will need to be made to simulate drug actions with high physiologic relevance. In summary, the device is a low cost option to test for hepatotoxicity in vitro under fluid flow.

Acknowledgement:

Financial support for this work was in part provided by the National Institutes of Health/National Center for Advancing Translational Sciences under grant No. UH2 TR000516-01, and by the National Science Foundation under grant No. CBET-1106153. This work was performed in part at the Cornell NanoScale Science and Technology Facility, a member of the National Nanotechnology Infrastructure Network, which is supported by the National Science Foundation (Grant ECS-0335765).

References:

1. N. Kaplowitz, *Nature Reviews Drug Discovery*, 2005, **4**, 489–499.
2. R. Kostadinova, F. Boess, D. Applegate, L. Suter, T. Weiser, T. Singer, B. Naughton, and A. Roth, *Toxicology and Applied Pharmacology*, 2013, **268**, 1–16.
3. B. D. Cosgrove, B. M. King, M. A. Hasan, L. G. Alexopoulos, P. A. Farazi, B. S. Hendriks, L. G. Griffith, P. K. Sorger, B. Tidor, J. J. Xu, and D. A. Lauffenburger, *Toxicology and Applied Pharmacology*, 2009, **237**, 317–330.
4. R. Gebhardt and D. Mecke, *Experimental cell research*, 1979, **124**, 349–359.
5. J. Dich and N. Grunnet, *Analytical Biochemistry*, 1992, **206**, 68–72.
6. P. Kan, H. Miyoshi, K. Yanagi, and N. Ohshima, *ASAIO Journal*, 1998, **44**, M441–M444.
7. P. Kan, H. Miyoshi, and N. Ohshima, *Tissue Engineering*, 2004, **10**, 1297–1307.
8. M. R. Ebrahimkhani, J. A. S. Neiman, M. S. B. Raredon, D. J. Hughes, and L. G. Griffith, *Advanced Drug Delivery Reviews*, 2014, **69-70**, 132–157.
9. L. De Bartolo, G. Jarosch-Von Schweder, A. Haverich, and A. Bader, *Biotechnology Progress*, 2000, **16**, 102–108.
10. L. De Bartolo, S. Salerno, S. Morelli, L. Giorno, M. Rende, B. Memoli, A. Procino, V. E. Andreucci, A. Bader, and E. Drioli, *Biomaterials*, 2006, **27**, 4794–4803.
11. B. Vinci, C. Duret, S. Klieber, S. Gerbal-Chaloin, A. Sa-Cunha, S. Laporte, B. Suc, P. Maurel, A. Ahluwalia, and M. Daujat-Chavanieu, *Biotechnology Journal*, 2011, **6**, 554–564.
12. L. Xia, S. Ng, R. Han, X. Tuo, G. Xiao, H. L. Leo, T. Cheng, and H. YU, *Biomaterials*, 2009, **30**, 5927–5936.
13. J. H. Sung, C. Kam, and M. L. Shuler, *Lab on a Chip*, 2010, **10**, 446–455.
14. P. M. van Midwoud, M. T. Merema, E. Verpoorte, and G. M. M. Groothuis, *Lab on a Chip*, 2010, **10**, 2778–2786.
15. S. Choi, O. Fukuda, A. Sakoda, and Y. Sakai, *Materials Science & Engineering C*, 2004, **24**, 333-339.
16. M. A. Guzzardi, F. Vozzi, and A. D. Ahluwalia, *Tissue Engineering Part A*, 2009, **15**, 3635–3644.
17. K. Viravaidya, A. Sin, and M. L. Shuler, *Biotechnology Progress*, 2004, **20**, 316–323.
18. K. Viravaidya and M. L. Shuler, *Biotechnology Progress*, 2004, **20**, 590–597.
19. Y. Y. Lau, Y.-H. Chen, T.-T. Liu, C. Li, X. Cui, R. E. White, and K.-C. Cheng, *Drug Metab. Dispos.*, 2004, **32**, 937–942.
20. C. Zhang, Z. Zhao, N. A. Abdul Rahim, D. van Noort, and H. Yu, *Lab on a Chip*, 2009, **9**, 3185–3192.
21. I. Wagner, E.-M. Materne, S. Brincker, U. Süßbier, C. Frädrich, M. Busek, F. Sonntag, D. A. Sakharov, E. V. Trushkin, A. G. Tonevitsky, R. Lauster, and U. Marx, *Lab on a Chip*, 2013, **13**, 3538–3547.
22. R. Brand, T. Hannah, C. Mueller, and Y. Cetin, *Annals of Biomedical Engineering*, 2000, **28**, 1210–1217.
23. G. J. Mahler, M. B. Esch, R. P. Glahn, and M. L. Shuler, *Biotechnology and bioengineering*, 2009,

104, 193–205.
24. J. H. Sung and M. L. Shuler, *Lab on a Chip*, 2009, **9**, 1385–1394.
25. D. A. Tatosian and M. L. Shuler, *Biotechnology and bioengineering*, 2009, **103**, 187–198.
26. M. B. Esch, G. J. Mahler, T. Stokol, and M. L. Shuler, *Lab on a Chip*, 2014, **14**, 3081–3092.
27. A. W. Tilles, H. Baskaran, P. Roy, M. L. Yarmush, and M. Toner, *Biotechnology and bioengineering*, 2001, **73**, 379–389.
28. A. Dash, M. B. Simmers, T. G. Deering, D. J. Berry, R. E. Feaver, N. E. Hastings, T. L. Pruett, E. L. LeCluyse, B. R. Blackman, and B. R. Wamhoff, *Am. J. Physiol., Cell Physiol.*, 2013, **304**, C1053–63.
29. C. M. Williams, G. Mehta, S. R. Peyton, A. S. Zeiger, K. J. Van Vliet, and L. G. Griffith, *Tissue Engineering Part A*, 2011, **17**, 1055–1068.

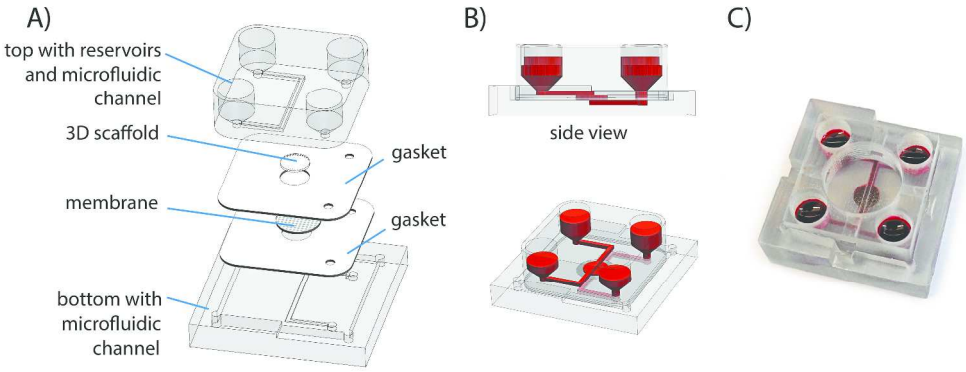

Figure 1: Schematic of device assembly and operation. The system consists of two silicone gaskets with 6 mm holes that serve as cell culture chambers (A). The silicone gaskets are sandwiched between two 3D printed plastic pieces that both provide fluidic channels. Medium that flows through the channels reach the cell culture from the top and the bottom (B-C). The device is placed on a rocker platform to create gravity-driven, periodically changing bidirectional medium flow.
401x153mm (300 x 300 DPI)

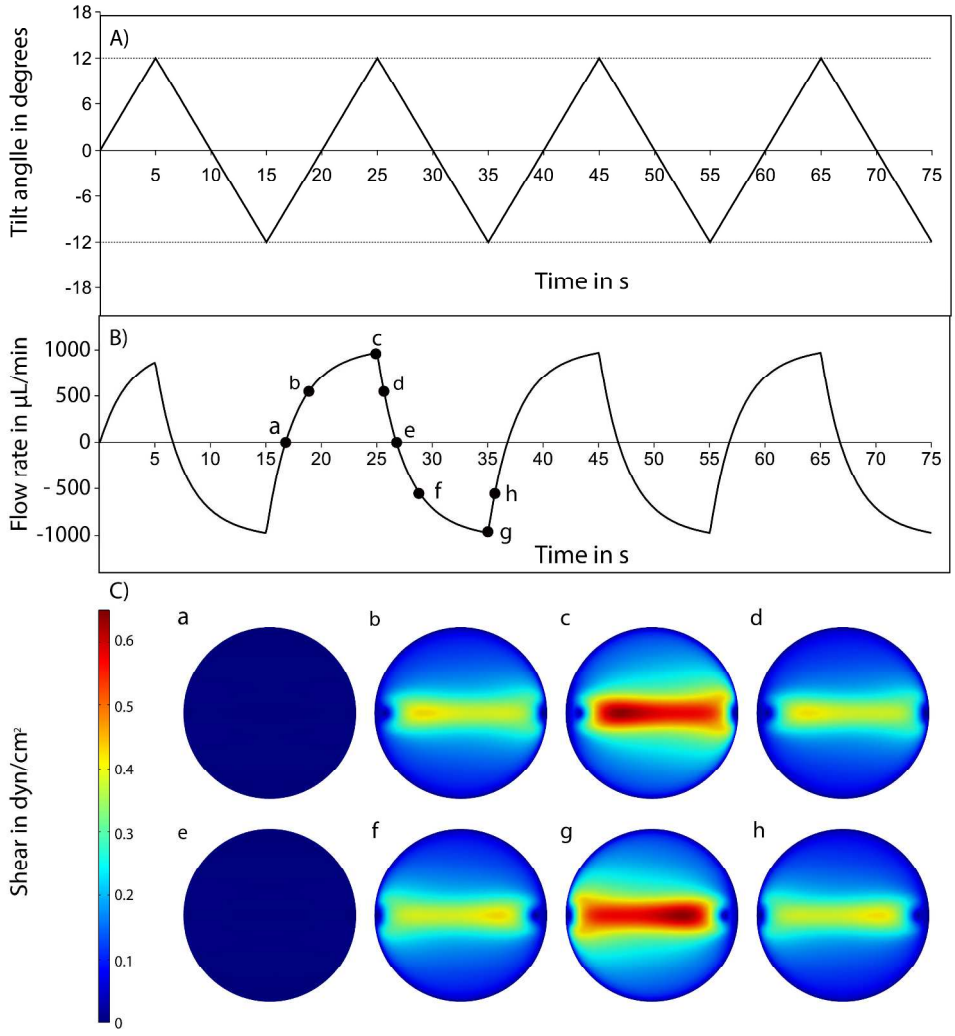

Figure 2: Fluorescence microscopy images of 3D cell cultures with scaffold and liver cells that were recovered from the cell culture device after 14 days of culture. Hepatocytes were immunostained against albumin (yellow) and are shown at magnifications of 4x (A), and 10x (B). The 3D scaffold is visible as a grid in blue. The cell cultures appear tissue-like with a high cell density. Stellate cells and Kupffer cells were stained for CD38 (green, shown in C) and CD68 (green, shown in D) using separate samples. Nuclei were stained with DAPI.

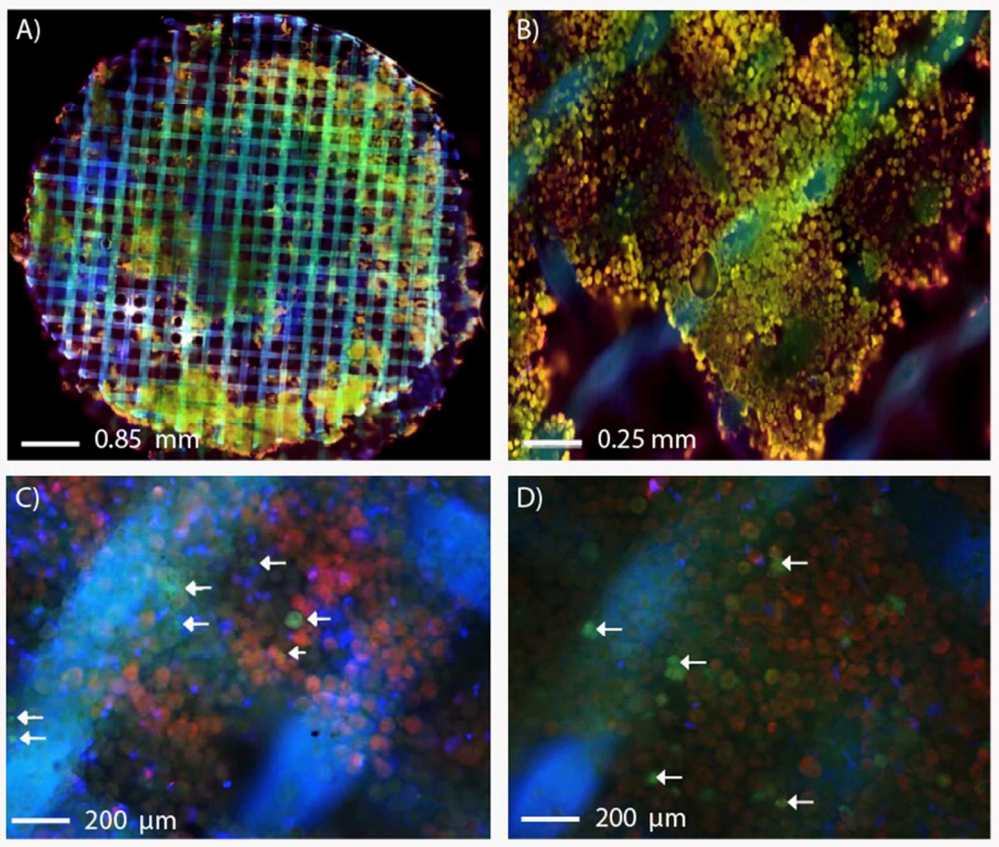

Figure 3: Rates of albumin (A) and urea (B) production throughout the 14-day culture period. Values are means ± standard deviations, n = 3 with each separate experiment consisting of six technical replicates. Significant differences (P>0.05) between static and dynamic cell culture conditions are indicated with an asterisk.
281x239mm (72 x 72 DPI)

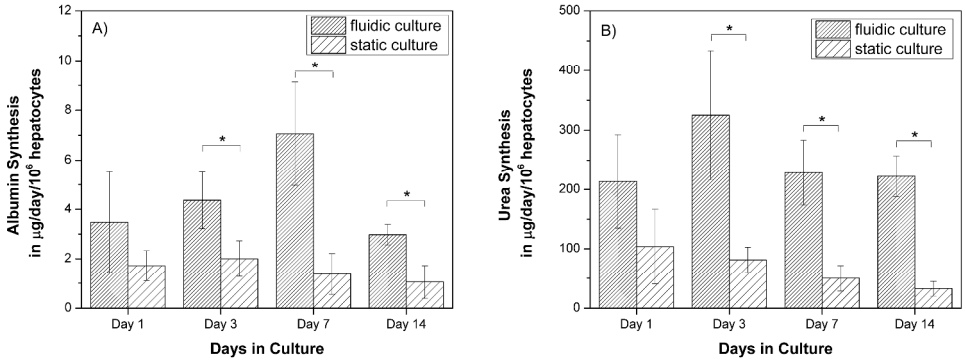

Figure 4: Activity of CYP 1A1 (A) and CYP 3A4 enzymes (B) throughout the 14-day cell culture period. Values are shown as percent increase compared to uninduced cultures. Values are means ± standard deviations, n = 3 with each separate experiment consisting of two technical replicates. Significant differences (P>0.05) between static and dynamic cell culture conditions are indicated with an asterisk.
498x207mm (300 x 300 DPI)

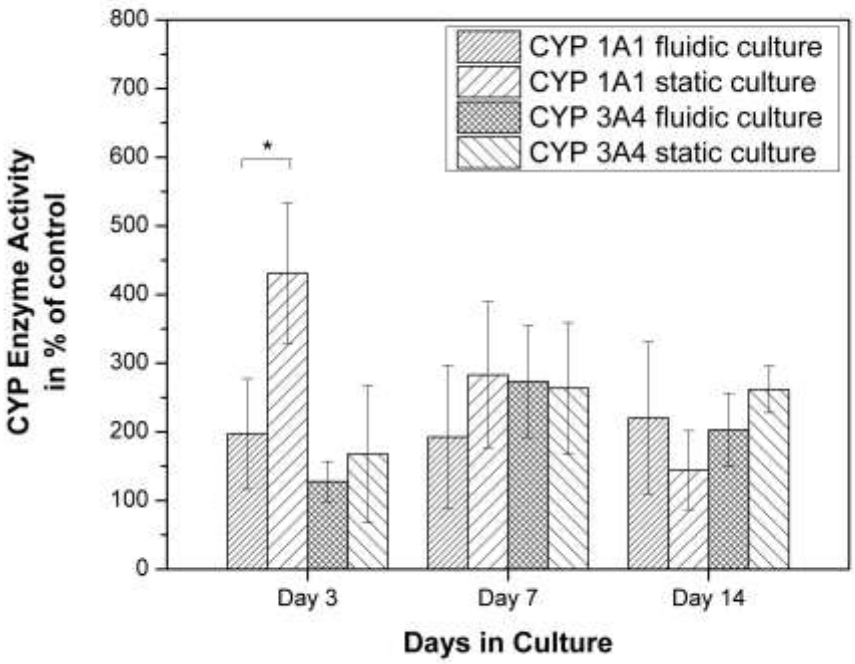

Figure 5: Concentrations of IL-8 in response to a 24-hour challenge with bacterial lipopolysaccharide (LPS). Values are means ± standard deviations, n = 3 with each separate experiment consisting of two technical replicates. Significant differences (P>0.05) between static and dynamic cell culture conditions are indicated with an asterisk.
207x158mm (300 x 300 DPI)

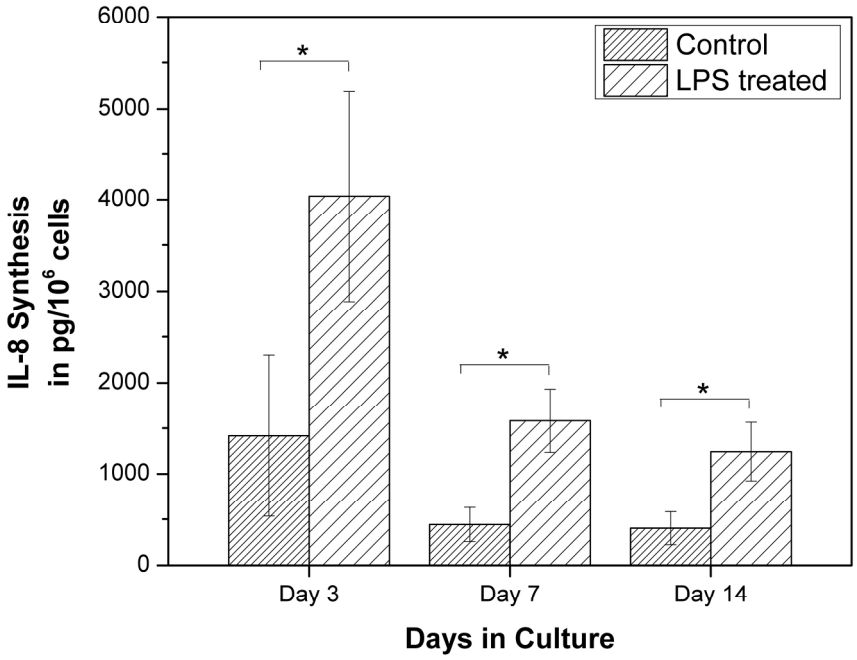

Figure 6: Results of theoretical simulation of the fluidic flow in the cell culture device. The flow velocity depends on the tilting angle (A) and oscillates (B). Shear stress is highest in the middle of the cell culture chamber (C). The letters a-h in (C) refer to tilting times and the corresponding flow rates marked in (B).
207x158mm (300 x 300 DPI)